CHEMISTRY OF MATERIALS

ARTICLE

pubs.acs.org/cm

Surface Reactions of μ^2-η^2-(^{t}Bu-acetylene)dicobalthexacarbonyl with Oxidized and H-terminated Si(111) Surfaces

Jinhee Kwon,*[,†] Mark Saly,[‡] Ravindra K. Kanjolia,[‡] and Yves J. Chabal[†]

[†]Materials Science and Engineering, the University of Texas at Dallas, Richardson, Texas 75080, United States

[‡]SAFC Hitech, Haverhill, Massachusetts 01832, United States

ABSTRACT: The reactions of a gas-phase metal carbonyl μ^2-η^2-(^{t}Bu-acetylene)-dicobalthexacarbonyl (CCTBA) with oxidized (SiO_2) and H-terminated (H/Si(111)) silicon surfaces at decarbonylation temperature (140 °C) are presented. Upon the first CCTBA exposure, the surface reactions strongly depend on the nature of the surfaces. On H/Si(111), metallic Si−Co bonds are formed after ∼80% of the Si−H bonds are consumed, and the carbonyl groups of the ligand form a stable structure of mixed $Co_2(CO)_6$ and semibridging CO. In contrast, Si−O−Co bonds are formed on SiO_2 at the outset, as confirmed by both IR absorbance spectra and Co 2*p* core-level XPS. Furthermore, carbonyls are not observed on SiO_2 after a completion of the first reaction, because of a weakening of their bond by the change of the Co oxidation state from Co^0 in CCTBA to Co^{2+} in Si−O−Co. On both substrates, the surface reaction of CCTBA gives rise to hydrosilylation, converting the alkyne group of the ligand into a C═C bond at the surface, which is very likely catalyzed by the presence of the cobalt carbonyl CCTBA itself. A cyclic CCTBA exposure of 2 s at 140 °C, followed by a 300 °C anneal, leads to metallic Co deposition on both H/Si(111) and SiO_2 surfaces, with Co thicknesses of 5 Å and 14 Å, respectively, after 15 cycles. After a few cycles, the surface chemistry changes, leading predominantly to the formation of enones together with (semi)bridging carbonyls.

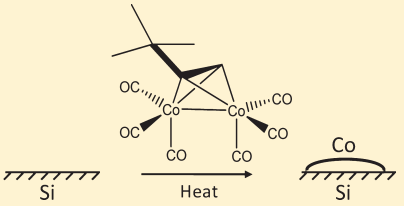

KEYWORDS: Coatings, thin films, and monolayers

1. INTRODUCTION

Metal carbonyl complexes are particularly important in organometallic chemistry, because of their increasing uses in homogeneous and heterogeneous catalysis[1,2] and polymerization reactions.[3,4] Reactions of metal carbonyls with surfaces are quite variable and strongly depend on the nature of surfaces such as acidity, basicity,[5,6] and surface defect density.[7,8] On metal oxide surfaces, metal carbonyls can form a simple Lewis acid−base adduct via bridging CO groups. Sublimation of $Co_2(CO)_8$ onto SiO_2 results in adsorption of cobalt carbonyl through hydrogen bonding between weakly acidic surface hydroxyl groups and oxygen atoms from bridging CO.[9] On dehydroxylated Al_2O_3, adduct formation takes place through the basic oxygen of a carbonyl interacting with a coordinatively unsaturated metal ion of the surface.[10]

The simple chemisorption characterized by these relatively well-defined surface species, however, does not hold at higher temperature regimes, where more complex reactions/transformations are involved. Thermal activation usually leads to decarbonylation and changes in the nuclearity and oxidation state. But, there has not been a systematic characterization of thermally activated organometallic chemistry on metal oxide and oxide-free surfaces.

This work focuses on surface reactions of gas-phase μ^2-η^2-(^{t}Bu-acetylene)dicobalthexacarbonyl (CCTBA) with oxidized and H-terminated Si surfaces at 140 °C, with subsequent characterization of the resulting Co films. The CCTBA precursor molecule has six carbonyl ligands with an alkyne group. This class of compounds is particularly interesting, because of its tendency to stabilize the alkyne group upon complexation.[11] The rich catalytic, electronic, and magnetic properties of cobalt make it very attractive for many industrial applications, as well as for fundamental research. Its catalytic properties have been widely utilized, especially in the well-known Fischer−Tropsch process of hydrogenation of carbon monoxide to hydrocarbon.[12] In microelectronics, the drive to scale down integrated circuitry (IC) has led to the consideration of cobalt silicide ($CoSi_2$) as a replacement for titanium silicide ($TiSi_2$) in future self-aligned silicide technology, because of its wider silicidation window and superior thermal and chemical stability.[13,14] Further interest in cobalt has been generated because of its magnetic property for data storage and prospective use in spintronics.[15] With all these potential applications involving metal deposition on silicon for microeletronic and magnetic devices and supported metal catalytic systems, the knowledge of the organometallic chemistry of metal carbonyls interaction with both oxidized and oxide-free Si surfaces is crucial for better understanding and control of these systems.

2. EXPERIMENTS AND RESULTS

Float-zone grown, double-side polished Si(111) substrates (lightly doped, $\rho \approx 10\ \Omega$ cm) with thin native oxide are cleaned by the standard RCA[16] method for oxide substrates. Atomically flat monohydride Si(111) surfaces (H/Si(111)) are obtained by etching in HF (∼20%, 30 s), followed by a 2-min dip in NH_4F

Received: October 21, 2010
Revised: December 13, 2010
Published: March 18, 2011

dx.doi.org/10.1021/cm103028x | *Chem. Mater.* 2011, 23, 2068–2074

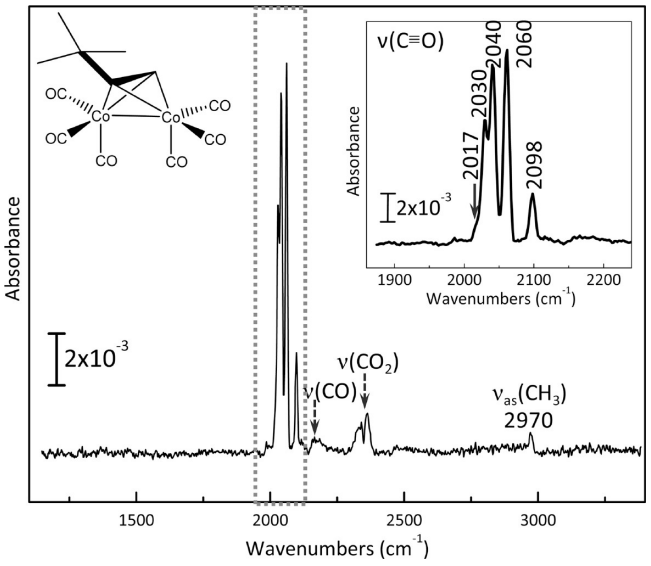

Figure 1. Infrared absorbance spectrum of gas-phase CCTBA ($P \approx 1.9$ Torr) (the molecular structure of CCTBA is shown as the inset at the upper left corner). The dotted rectangular region corresponds to the carbonyl (CO) stretching vibrations, which is expanded as the inset for clarification. Byproducts of dissociated CCTBA are indicated by dotted arrows (i.e., CO and CO_2).

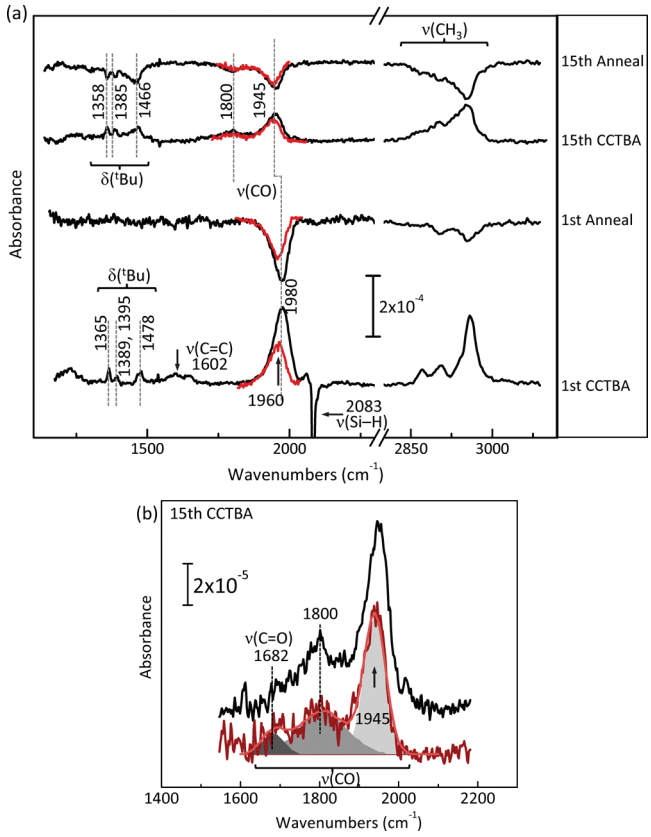

Figure 2. (a) Differential spectra of H/Si(111) recorded at the Brewster angle, after the 1st and 15th cycle of CCTBA exposure (2-s pulse) at 140 °C and annealing at 300 °C, referenced to each preceding treatment. The red spectra of the CO stretching modes are measured at near-normal incidence. (b) Details of ν(CO) stretching absorption spectra after the 15th CCTBA exposure measured at the Brewster angle (top spectrum) and at near-normal incidence, where three shaded peaks show fitted results (bottom spectrum).

(~49%).[17] After a thorough rinsing with deionized water and blow drying with nitrogen (N_2), the sample is loaded in the reactor with the base pressure of 10^{-4} Torr. CCTBA is heated up to 45 °C and a 2-s CCTBA pulse is carried into a reactor by ultrapure N_2 (flow rate = 100 sccm, $P \approx 300$ mTorr). During exposure, the Si substrate is kept at 140 °C. The sample is then heated up to 300 °C in N_2 ambient ($P \approx 10$ Torr) to remove surface ligands left after the previous CCTBA reaction. The cycles of CCTBA exposure and annealing are repeated to investigate and distinguish the reaction chemistry at the interface region close to the substrate and on the growing Co film surface where different surface reactions are expected. In situ infrared absorbance spectroscopy is carried out after every CCTBA exposure and annealing, using a Thermo Nicolet 6700 interferometer that is coupled to the reactor via external optics. A single-pass transmission geometry is used with an incidence angle close to the Brewster angle and normal incidence, to help distinguish polarization of infrared vibrational modes in absorbance spectra.[18,19] Investigation of oxidation states of cobalt and surface morphology is carried out using X-ray photoemission spectroscopy (XPS) and atomic force microscopy (AFM), respectively.

2.1. Infrared Absorption Spectra of Gas-Phase CCTBA. Before surface reactions are studied, the integrity or possible degradation of the precursor before and during pulsing in the reactor is examined. Figure 1 shows IR absorbance spectrum of gas-phase CCTBA (1.9 Torr) before a Si sample is loaded in the reactor. In metal carbonyls, the number of C≡O stretching modes increases with the number of CO ligands and is subject to the symmetry of the metal complex. It is therefore expected that $Co_2(CO)_6(RC{\equiv}CR')$ complexes have 5 or 6 absorptions in the carbonyl region, which vary as a function of R and R′ substituents.[20] The CCTBA ($Co_2(CO)_6{}^tBuC{\equiv}CH$) molecule possesses strong C≡O stretching modes at 2030, 2040, 2060, and 2098 cm^{-1} and a shoulder at 2017 cm^{-1} (see the inset of Figure 1), and these frequencies are almost identical to those reported for $Co_2(CO)_6CH{\equiv}CH$ characterized by C_{2v} symmetry.[21] The band at 2970 cm^{-1} corresponds to the asymmetric stretching of CH_3 from the ^{t}Bu groups of the ligand. Except for these strong CO and CH_3 stretching vibrations, modes with weak intensity such as ν(CH) (~3100 cm^{-1}), ν(C≡C) (1490−1630 cm^{-1}),[22−26] and Co−C (500−600 cm^{-1})[21] are not observed in Figure 1. On the other hand, the presence of the doublets of gas-phase CO ($\nu_{as}(CO)$ = 2143 cm^{-1}) and CO_2 ($\nu_{as}(CO_2)$ = 2349 cm^{-1}) suggests that there is partial dissociation of the precursor inside the ampule or the reactor.

2.2. Surface Reactions of CCTBA with H/Si(111). After H/Si(111) is exposed to the first CCTBA pulse at 140 °C, a quite intense ν(CO) mode is observed at 1980 cm^{-1} on the surface (Figure 2a, spectrum labeled as "1st CCTBA"). This frequency is lower than that of linear carbonyl species on Co^0 (ν(CO) > 2050 cm^{-1}) or on oxidized Co^{n+} (ν(CO) = 2140−2190 cm^{-1}) and higher than CO adsorbed on multifold sites (ν(CO) ≈ 1810 cm^{-1}).[27] According to Bitterwolf et al.,[28] photolysis or thermal decomposition of $Co_2(CO)_6$(alkyne) complexes leads to the formation of $Co_2(CO)_n$(alkyne) (n = 4 or 5) derivatives that are characterized by several ν(CO) modes above 2000 cm^{-1}. There are no modes above 2000 cm^{-1} associated with ν(CO) in the IR

dx.doi.org/10.1021/cm103028x |Chem. Mater. 2011, 23, 2068–2074

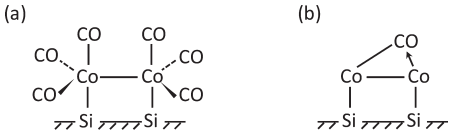

Figure 3. Potential carbonyl structure of (a) $Co_2(CO)_6$ and (b) semibridging CO after the first CCTBA exposure to H/Si(111), corresponding to CO stretching absorption at 1980 (1960) cm^{-1} measured at Brewster (normal) incidence.

absorption spectra in Figure 2a, indicating the absence of $Co_2(CO)_n$− (n = 4 or 5) structures at the surface.

A single CO stretching mode at 1980 cm^{-1} is possible when dicobalt carbonyl complexes have the point group D_{3d}, which would give rise to only one IR active absorption from two CO stretching modes with A_{1g} and E_g character.[29,30] If we ignore the alkyne ligands coordinated to Co when adsorbed on the surface, the structure of $(Co(CO)_3)_2$ bonded to surface Si atoms (see Figure 3a) has approximately D_{3d} symmetry, which is consistent with the CO stretching observed at 1980 cm^{-1} (Brewster angle) and 1960 cm^{-1} (near-normal incidence) in Figure 2a. The integrated area under the CO stretching mode centered at 1960 cm^{-1} measured with the near-normal incidence is ∼52% of that measured at the Brewster angle, indicating that a fraction of the CO groups are oriented in the plane parallel to the surface, as shown in Figure 3a.

Another possible assignment of the ν(CO) mode in the spectrum recorded after the first CCTBA exposure is associated with a configuration involving semibridging asymmetric CO groups (Figure 3b). The ν(CO) band is asymmetric with a broad tail toward the lower frequency, suggesting that there is another type of CO configuration on the surface. Lagunas et al. reported ν(CO) absorption at 1945 cm^{-1} associated with a decomposition product of $CO_4(CO)_{12}$. They used DFT calculations to assign it to semibridging CO on Co−Co.[31] It is most likely that both the $(Co(CO)_3)_2$ and semibridging CO structures shown in Figure 3 are present on the surface after the first CCTBA exposure. All carbonyl groups on the surface are removed after annealing at 300 °C, as evidenced by an intensity loss of the ν(CO) mode in the region 1900−2000 cm^{-1} in Figure 2a (first anneal). This observation is consistent with the observation that CO groups can be easily desorbed at moderate temperatures (∼300 °C).

The CCTBA molecule is very reactive with H/Si(111), consuming ∼80% of surface hydrogen after the first exposure according to the loss of integrated area of the ν(Si−H) mode at 2083 cm^{-1}. Rutherford backscattering spectrometry (RBS) measurements indicate that the cobalt surface density is 5.5 × 10^{14} Co atoms/cm^2 after the first CCTBA exposure; i.e., ∼ 70% of the initial H density (7.8 × 10^{14} H atoms/cm^2) on Si(111). This observation is consistent with a one-to-one Co−Si bond formation, as shown in Figure 3, although it does not unambiguously show that every Co atom is linked to Si. The remaining 10% of reacted Si−H sites are occupied by other species, most likely Si−C bonds.

Absorption features in the 2700−3000 cm^{-1} (CH_3 stretching) and the 1350−1500 cm^{-1} (deformation) regions indicate that t-butyl species are present on the surface after the first CCTBA exposure. In particular, the modes at 1365 cm^{-1} and doublets near 1390 and 1478 cm^{-1} are typical of t-butyl symmetric and asymmetric deformations. In contrast to a complete desorption

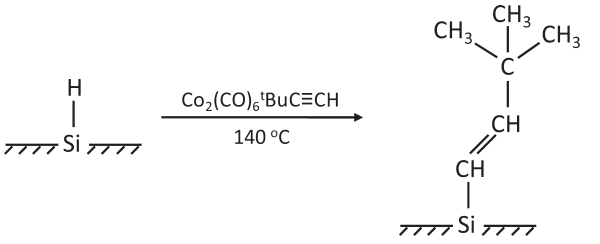

Figure 4. Possible surface species bound by a Si−C− linkage after the first surface reaction of $Co_2(CO)_6{}^tBuC{\equiv}CH$ with H/Si(111).

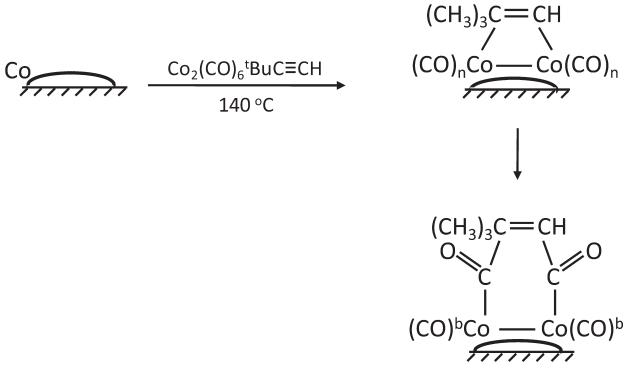

Figure 5. Possible surface species after the surface is mostly covered with Co. $(CO)^b$ indicates semibridging or bridging carbonyls.

of CO after annealing at 300 °C, the losses of $\nu(CH_3)$ in 2700−3000 cm^{-1} and $\delta(^tBu)$ in 1350−1500 cm^{-1} after the first annealing are relatively weaker than the initial intensities recorded after the first CCTBA exposure (Figure 2a). This indicates that t-butyl ligands may be bound to the surface through strong Si−C bonds that remain stable during a 300 °C annealing. The small intensity loss after annealing can result from desorption of some residual t-butyl ligands bound to Co on the surface. Figure 4 shows a possible t-butyl moiety bound on the surface by a Si−C linkage after the first CCTBA exposure.

Hydrosilylation (i.e., bond formation between the terminal alkyne to the Si(111) surface), shown in Figure 4, is known to readily occur via thermal activation.[32−34] Moreover, the presence of the cobalt carbonyl complex can act as a catalyst to induce hydrosilylation. The mode at 1602 cm^{-1} after the first CCTBA in Figure 2a is characteristic of the C═C stretching absorption, suggesting that hydrosilylation on the surface has taken place, converting the alkyne group into alkene.

After several CCTBA and annealing cycles, a different surface chemistry is expected, because the substrate becomes more fully covered by a Co film, leaving less and less surface hydrogen available for reaction with CCTBA. At the 15th cycle, for example, the t-butyl deformation modes in 1300−1500 cm^{-1} and C−H stretching in 2700−3000 cm^{-1} are slightly shifted in frequency (see Figure 2a, "15th CCTBA"), indicating that the bonding environment around the t-butyl moiety has changed. The CO stretching absorption is now dominated by semibridging CO at 1945 cm^{-1} and bridging CO at 1800 cm^{-1}. Polarization-dependent data obtained using Brewster and near-normal incidence indicate that these CO modes are oriented mostly parallel to the surface. The CO stretching region in Figure 2b shows a broad tail below 1800 cm^{-1} after the 15th CCTBA exposure.

dx.doi.org/10.1021/cm103028x |*Chem. Mater.* 2011, 23, 2068–2074

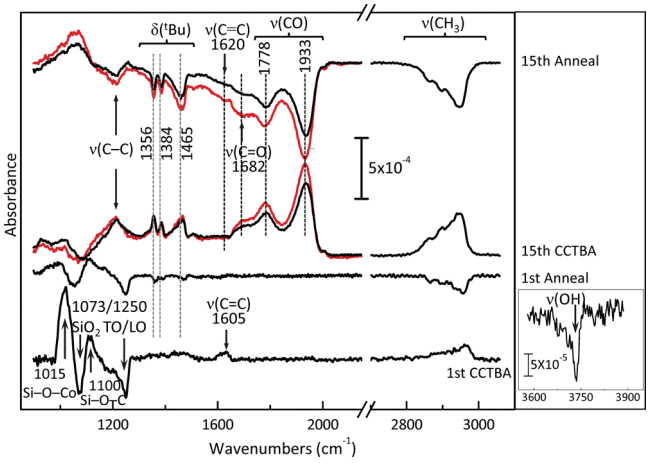

Figure 6. Differential spectra of the oxidized silicon surface (SiO_2) after the 1st and 15th cycles (1 cycle = CCTBA exposure at 140 °C and annealing at 300 °C), referenced to each preceding treatment measured at Brewster angle. The red spectra of the 15th cycle are measured at near-normal incidence. The inset highlights the −OH stretching absorption region after the first CCTBA exposure.

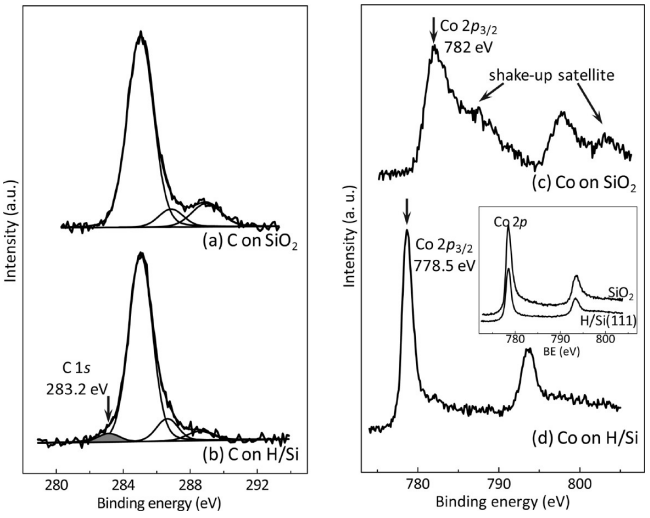

Figure 7. XPS of the C 1*s* and Co 2*p* core levels, respectively, on (a, c) SiO_2 and (b, d) H/Si(111) after the first CCTBA exposure at 140 °C. The inset is Co 2*p* XPS after 15 cycles of CCTBA exposure and 300 °C annealing, measured after the oxidized surface has been removed by Ar sputtering.

It is evident that there is another mode near at 1682 cm^{-1} best observed in the near-normal incidence spectrum in Figure 2b, which is typical of a C═O stretching vibration. The presence of C═O at ∼1682 cm^{-1}, together with C≡O modes at 1800 and 1945 cm^{-1}, suggests that enone groups, consisting of alkenes and ketones, are formed on the surface after Co films are deposited. Figure 5 shows a schematic of possible pathways for enone formation on Co films.

At the 15th CCTBA exposure, the surface is mostly covered with Co, and the surface reaction is dominated by decarbonylation where all the CO groups are removed, except for bridging (1800 cm^{-1}) and/or semibridging (1945 cm^{-1}) carbonyls. In particular, the absorption at 1980 cm^{-1}, corresponding to the $Co_2(CO)_6$ structure, is no longer observed after the 15th CCTBA exposure. The dominating decarbonylation reaction and the presence of Co film underneath acting as a catalyst can foster the insertion of CO between Co and alkyne C atoms. This process is analogous to what occurs during hydroformylation, resulting in the formation of C═O groups on the surface. All these surface species are completely desorbed after 300 °C annealing, as shown in Figure 2a in the spectrum labeled "15th Anneal."

2.3. Surface Reactions of CCTBA with SiO_2. Figure 6 shows surface infrared differential spectra of SiO_2 measured after the 1st and 15th cycles of CCTBA exposure at 140 °C and annealing at 300 °C. The loss of ν(OH) at 3735 cm^{-1} (inset) after the first CCTBA exposure indicates that the reaction between the initial SiO_2 and CCTBA is mainly through the hydroxyl groups on the surface. The integrated area under the −OH stretching mode, compared with well-characterized OH + H monolayer on Si(100) as calibration,[19,35,36] suggests that the first CCTBA pulse completely consumes hydroxyl groups on the surface. The reaction slightly disrupts the interatomic bonding of the underlying Si−O lattices,[37] resulting in the loss of the transverse (TO) and longitudinal optical (LO) modes of SiO_2 at 1073 and 1250 cm^{-1}. The appearance of modes at 2800−3000 cm^{-1} and 1300−1500 cm^{-1} region, corresponding to the stretching and deformation of *t*-butyl CH_3, respectively, is associated with the presence of methyl groups from the ligand as a surface species after the reaction. A strong band at 1015 cm^{-1} is assigned to Si−O−Co bonds,[38] indicating that Co is directly coordinated to a surface oxygen.

The mode at 1100 cm^{-1} is assigned to (Si−)O−C stretching,[39] suggesting that a part of ^{t}BuC≡CH ligands are transferred to the surface, forming Si−O−C bonds, similar to what is observed on H/Si(111). The ^{t}BuC≡CH part of CCTBA reacts with hydroxyl groups, forming Si−O−CH═CH−, as evidenced by the presence of C═C stretching vibration at 1605 cm^{-1}. In contrast to *t*-butyl moiety bound through Si−C on H/Si(111), *t*-butyl groups on SiO_2 are completely desorbed after a 300 °C anneal, as evidenced by a negative absorption of the deformation and stretching vibrations of *t*-butyl species in the differential spectrum measured after the first annealing in Figure 6.

The presence of carbonyl groups on SiO_2 after the first CCTBA exposure is negligible, in contrast to what is observed on H/Si(111). After the second cycle (data not shown), however, the adsorption of the ligands is stronger than what is observed on H/Si(111) of the same number of cycles. At the 15th CCTBA exposure, the integrated areas under $\nu(CH_3)$ and ν(CO) on SiO_2 in Figure 6 are almost twice as much as those of the 15th CCTBA exposure on H/Si(111) in Figure 2a. The intensity of the skeletal vibration (C−C stretching) of *t*-butyl near 1200−1260 cm^{-1} is also strong. The modes at 1933 and 1778 cm^{-1} are assigned to the semibriging and bridging CO, respectively. The presence of the stretching vibrations of C═O at 1682 cm^{-1} and C═C at 1620 cm^{-1} indicates that the CCTBA is converted into a structure similar to what is shown in Figure 5. The stronger intensity makes it possible to distinguish ν(C═C) at 1620 cm^{-1}, which is not apparent in Figure 2a.

2.4. Chemical States and Morphology of Cobalt Film. XPS measurements after the first CCTBA exposure reveal the presence of an additional C 1*s* component with a binding energy of 283.2 eV on H/Si(111) (Figure 7b), which is lower than that of aliphatic and adventitious carbon at 285 eV. This lower binding

dx.doi.org/10.1021/cm103028x |*Chem. Mater.* 2011, 23, 2068–2074

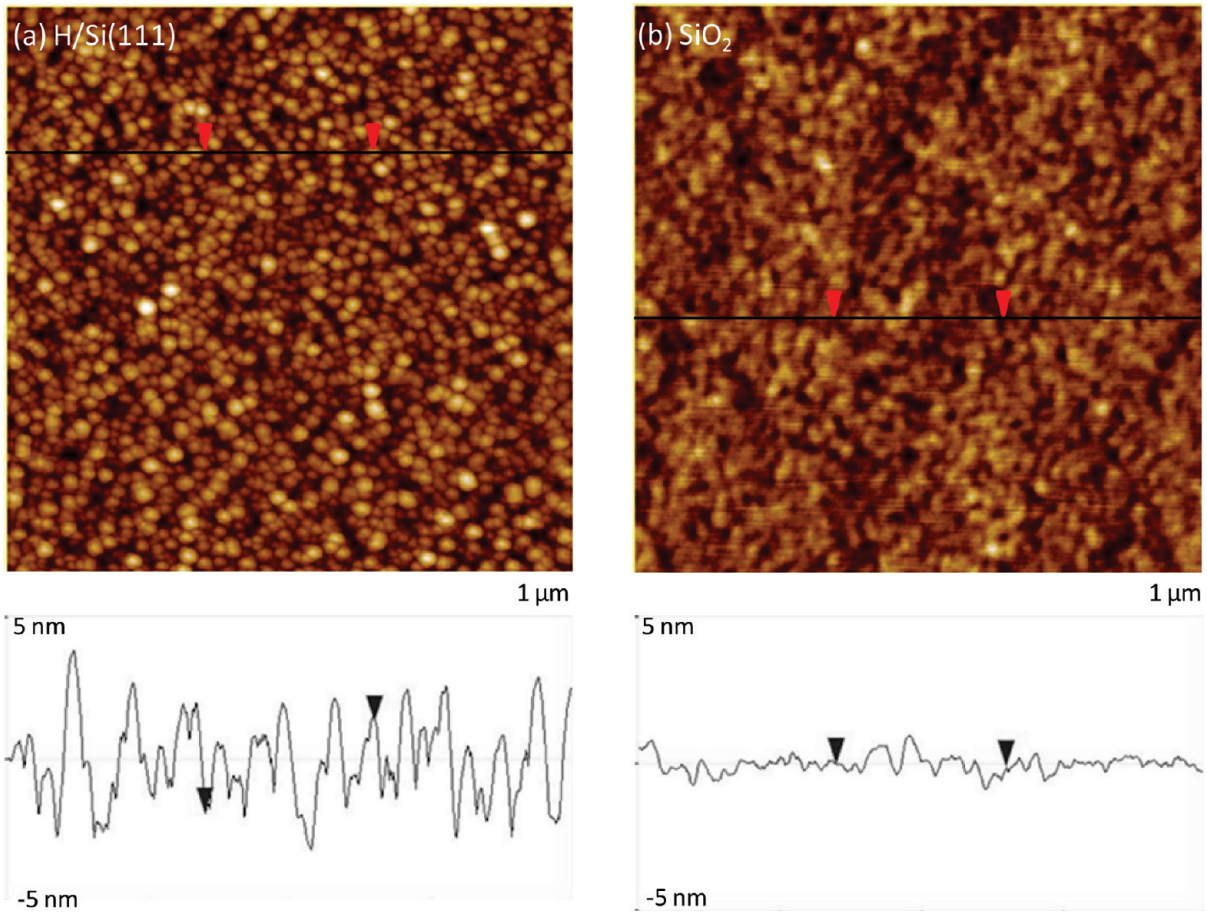

Figure 8. AFM surface images of (a) H/Si(111) and (b) SiO_2 after 15 cyclic exposures of CCTBA, followed by annealing at 300 °C and line profiles at the location of the sections.

energy component is attributed to C atoms chemically bound to Si atoms, which is consistent with the IR absorbance spectra in Figure 2, as described above.[40,41] This lower binding energy component of C 1*s* is absent on SiO_2, as shown in Figure 7a. The presence of Co^{2+} on SiO_2 is confirmed by Co $2p_{3/2}$ binding energy at 782 eV with a relatively intense 3d → 4s shakeup satellite at 787.5 eV and spin-orbit splitting of 16 eV between Co $2p_{3/2}$ and $2p_{1/2}$ in Figure 7c[42]. This is also consistent with Si−O−Co covalent bond formation observed in IR absorbance in Figure 6. In contrast, the Co 2*p* on H/Si(111) (Figure 7d) is located at a lower binding energy (778.5 eV) with a spin-orbit splitting of 14.9 eV, which is characteristic of metallic Co^0. Even with these different oxidation states for Co on H/Si(111) and SiO_2 after the first CCTBA exposure, the configuration of Co grown after 15 cycles of CCTBA exposure and annealing is characterized by the same core level energy (Co $2p_{3/2}$ at 778.5 eV) on both surfaces (inset of Figure 7), indicating that metallic Co^0 is deposited during the process regardless of the initial reactions with the substrate.

AFM images in Figure 8 measured after 15 cycles show that the morphology is substantially different between H/Si(111) and SiO_2 substrates. The root-mean-square (rms) roughness of the Co films (see Figure 8a) is 1.2 nm on H/Si(111), whereas, on SiO_2, the rms roughness is only 0.3 nm (see Figure 8b). The dispersion of grain size of Co on H/Si(111) is quite small, with an average size of 20−25 nm, according to the section analysis in Figure 8a, which suggests Co island formation on H/Si(111).

DISCUSSION

The hydroxyl groups on the SiO_2 surface constitute mildly Brønsted acidic sites that act as adsorption sites for carbonyl precursors.[43] If there is hydrogen bond formation between surface −OH and CCTBA, the intensity of the band at 3735 cm^{-1} would be expected to shift to ~3650 cm^{-1}.[44,45] This is not the case with the substrate temperature at 140 °C, as shown in Figure 6, where only the loss of the mode at 3735 cm^{-1} is observed. Moreover, the absence of CO stretching vibration indicates that the decarbonylation is complete, leaving no carbonyl species on the SiO_2 surface after the first CCTBA exposure. It is known that thermally activated reactions between a metal carbonyl complex and an oxide surface depend on the nature of the oxide. For example, it was reported that there is a gradual loss of CO from $Cr(CO)_6$ on Al_2O_3 surfaces. In contrast, all six CO ligands of $Cr(CO)_6$ are removed in rapid succession over a narrow temperature range on SiO_2 surfaces.[46] Similarly, the absence of CO on SiO_2 after the first CCTBA exposure in Figure 6 can be attributed to a lack of stabilization of subcarbonyl species after reaction of CCTBA on SiO_2. The strength of a Co−CO bond with Co in a +2 oxidation state (i.e., Si−O−Co) is naturally weakened, because of the decrease of electron density at the metal center. Such decomposition of a carbonyl complex with evolution of carbon monoxide, hydrogen, and sometimes hydrocarbons is well documented by temperature-programmed decomposition studies.[47]

dx.doi.org/10.1021/cm103028x |*Chem. Mater.* 2011, 23, 2068–2074

In contrast to SiO_2, the first exposure of CCTBA to H/Si(111) leads to the formation of Si−Co bonds with carbonyls in D_{3d} symmetry, such as that obserevd in $Co_2(CO)_6$ or semibridging CO, emphasizing the dependence of CO stability on the nature of the substrate surface.

Interestingly, the C═C stretching absorption at ∼1600 cm^{-1} is observed both on H/Si(111) (Figure 2a) and on SiO_2 (Figure 6) after the first CCTBA exposure, suggesting that hydrosilylation readily takes place on both surfaces. The presence of cobalt carbonyls, which are known to catalyze the activation of alkynes to surface-bound alkenes, may therefore play a role in hydrosilylation during surface reactions.

At later cycles (e.g., the 15th cycle), where no more surface adsorption sites are available, the reaction of CCTBA with the deposited Co films induces enone formation. It has been observed that dicobalt carbonyl complexes react with acetylene and CO_2 in solution to produce cyclic enones.[48] The strong intensity of ν(C═O) and ν(C═C) in Figure 6 suggests that enones are formed through surface reactions of CCTBA, similar to what occurs in solution. The geometric and chemical characteristics of CCTBA can be changed through multicenter interaction at the surface, which might play a role in increasing the stability of intermediate transition states during CO insertion between the Co−C bonds of CCTBA on the surface. As carbonyls are partially converted into enone groups on the surface, the remaining CO favors a semibridging structure. Semibridging CO can be considered as the normal terminal CO bonded to a metal that is interacting both with CO and with one or more other metal centers. Its presence helps to equalize charge on the metal centers by donating electron density from the metal d orbitals into the 2π (π^*) orbital of the CO group.[49] Theoretical calculations show that decarbonylation of poly Co species favors the formation of CO ligands in semibridging geometry.[31]

The distinct film morphology after 15 cycles shown in Figure 8 can be related to the different film thickness. The thickness of Co on H/Si(111) and SiO_2 measured by RBS after 15 cycles is ∼5 and 14 Å, respectively. The rougher morphology on H/Si(111) thus suggests that the film is still in the nucleation phase. The higher Co film growth rate on SiO_2 can be easily expected from the higher absorption intensities in Figure 6. The higher growth rate on SiO_2 seems to be activated sometime after the second CCTBA exposure, because the first exposure deposits the same amount of Co atoms both on SiO_2 and H/Si(111) according to RBS. The difference may be due to the nature of the surface reaction products during the first few cycles, leading to chemical and morphological differences and, therefore, different growth rates. For SiO_2 surfaces, the organic ligands left on the surface after the first CCTBA exposure are almost completely removed by the subsequent annealing at 300 °C (Figure 6). For H/Si(111) surfaces, a fraction of the ligands transferred to Si to form Si−C bonds after the first CCTBA pulse remain after annealing at 300 °C (Figure 2a), resulting in a surface that contains more C atoms than on the SiO_2 surfaces after the first anneal. These organic fragments on the H/Si(111) surfaces decrease the number of available reaction sites during the second CCTBA exposure. This C-rich area will not be available for further CCTBA reactions, resulting in a lower growth rate, as well as more island-type growth, as observed in the AFM image in Figure 8a.

In summary, the surface reactions of CCTBA with oxidized and H/Si(111) surfaces have been investigated. Although carbonyl groups are quite stable on H/Si(111) in the form of $Co_2(CO)_6$ and semibridging CO after the first CCTBA exposure, the presence of surface bound CO is negligible on SiO_2, because of the weakening of the bond strength caused by the change in the oxidation state of the metal center. The presence of C═C after the initial surface reaction suggests that the alkyne group is converted to surface bound alkene through hydrosilylation catalyzed by cobalt carbonyls. During cyclic exposure of CCTBA and annealing at 300 °C, metallic Co is deposited on both surfaces, except for the very initial Co^{2+} of Si−O−Co on SiO_2. The reaction of CCTBA with deposited Co films is dominated by the formation of enone groups, together with (semi)bridging carbonyls on the surface. Co films are characterized by an island structure with the grain size of 20−25 nm on H/Si(111), but are more homogeneous, with an rms roughness of only 0.3 nm on SiO_2 after 15 cycles.

AUTHOR INFORMATION

Corresponding Author
*E-mail: jinhee@utdallas.edu.

ACKNOWLEDGMENT

This work was supported partly by SAFC Hitech and NSF (CHE-0911197).

REFERENCES

(1) Brisdon, B. J.; Griffin, G. F.; Pierce, J.; Walton, R. A. *J. Organomet. Chem.* **1981**, *219* (1), 53–59.
(2) King, R. B.; King, A. D. *Russ. Chem. Bull.* **1994**, *43* (9), 1445–1450.
(3) Masuda, T.; Kuwane, Y.; Yamamoto, K.; Higashimura, T. *Polym. Bull.* **1980**, *2* (12), 823–827.
(4) Xu, K.; Peng, H.; Lam, J. W. Y.; Poon, T. W. H.; Dong, Y.; Xu, H.; Sun, Q.; Cheuk, K. K. L.; Salhi, F.; Lee, P. P. S.; Tang, B. Z. *Macromolecules* **2000**, *33* (19), 6918–6924.
(5) Correa, F.; Nakamura, R.; Stimson, R. E.; Burwell, R. L.; Shriver, D. F. *J. Am. Chem. Soc.* **1980**, *102* (15), 5112–5114.
(6) Uchiyama, S.; Gates, B. C. *Inorg. Chim. Acta* **1988**, *147* (1), 65–70.
(7) Zecchina, A.; Platero, E. E.; Arean, C. O. *J. Mol. Catal.* **1988**, *45* (3), 373–379.
(8) Zecchina, A.; Escalona Platero, E.; Otero Arean, C. *Inorg. Chem.* **1988**, *27* (1), 102–106.
(9) Suvanto, S.; Pakkanen, T. A.; Backman, L. *Appl. Catal., A* **1999**, *177* (1), 25–36.
(10) Tessier-Youngs, C.; Correa, F.; Pioch, D.; Burwell, R. L.; Shriver, D. F. *Organometallics* **1983**, *2* (7), 898–903.
(11) Went, M. J.; Stone, F. G. A.; Robert, W. In *Advances in Organometallic Chemistry*; Academic Press: New York, 1997; Vol. 41, pp 69−125.
(12) *Fischer−Tropsch Technology*; Elsevier: Amsterdam, 2004; Vol. 152.
(13) Hsia, S. L.; Tan, T. Y.; Smith, P.; McGuire, G. E. *J. Appl. Phys.* **1992**, *72* (5), 1864–1873.
(14) Lindsay, R.; Lauwers, A.; de Potter, M.; Roelandts, N.; Vrancken, C.; Maex, K. *Microelectron. Eng.* **2001**, *55* (1−4), 157–162.
(15) Yakovlev, N.; Kaveev, A.; Sokolov, N.; Krichevtsov, B.; Huan, A. *Curr. Appl. Phys.* **2006**, *6* (3), 575–578.
(16) Higashi, G. S.; Chabal, Y. J. In *Handbook of Silicon Wafer Cleaning Technology: Science, Technology, and Applications*; Kern, W., Ed.; William Andrew Publishing: 1994.
(17) Higashi, G. S.; Chabal, Y. J.; Trucks, G. W.; Raghavachari, K. *Appl. Phys. Lett.* **1990**, *56* (7), 656–658.

(18) Stefanov, B. B.; Gurevich, A. B.; Weldon, M. K.; Raghavachari, K.; Chabal, Y. J. *Phys. Rev. Lett.* **1998**, *81* (18), 3908.
(19) Gurevich, A. B.; Stefanov, B. B.; Weldon, M. K.; Chabal, Y. J.; Raghavachari, K. *Phys. Rev. B* **1998**, *58* (20), R13434.
(20) Bor, G.; Kettle, S. F. A.; Stanghellini, P. L. *Inorg. Chim. Acta* **1976**, *18*, L18–L20.
(21) Iwashita, Y.; Tamura, F.; Nakamura, A. *Inorg. Chem.* **1969**, *8* (5), 1179–1183.
(22) Stanghellini, P. L.; Rossetti, R. *Inorg. Chem.* **1990**, *29* (11), 2047–2052.
(23) Meyer, A.; Bigorgne, M. *Organometallics* **1984**, *3* (7), 1112–1118.
(24) Evans, J.; McNulty, G. S. *J. Chem. Soc. Dalton Trans.* **1984**, 79.
(25) Bandy, B. J.; Chesters, M. A.; Pemble, M. E.; McDougall, G. S.; Sheppard, N. *Surf. Sci.* **1984**, *139* (1), 87–97.
(26) Avery, N. R. *J. Am. Chem. Soc.* **1985**, *107* (23), 6711–6712.
(27) Yu, L.-h.; Zhang, S.-m.; Guo, X.; Wang, D.; Wang, S.-r.; Wu, S.-h. *Central Eur. J. Chem.* **2007**, *5* (1), 144–155.
(28) Bitterwolf, T. E.; Scallorn, W. B.; Weiss, C. A. *J. Organomet. Chem.* **2000**, *605* (1), 7–14.
(29) Douglas, B. E.; McDaniel, D. H.; Alexander, J. J. *Concepts and Models of Inorganic Chemistry*, 3rd Edition; Wiley: New York, 1994.
(30) Friedel, R. A.; Wender, I.; Shufler, S. L.; Sternberg, H. W. *J. Am. Chem. Soc.* **1955**, *77* (15), 3951–3958.
(31) Lagunas, A.; Jimeno, C.; Font, D.; Solà, L.; Pericàs, M. A. *Langmuir* **2006**, *22* (8), 3823–3829.
(32) Linford, M. R.; Fenter, P.; Eisenberger, P. M.; Chidsey, C. E. D. *J. Am. Chem. Soc.* **1995**, *117* (11), 3145–3155.
(33) Sieval, A. B.; Demirel, A. L.; Nissink, J. W. M.; Linford, M. R.; van der Maas, J. H.; de Jeu, W. H.; Zuilhof, H.; Sudhölter, E. J. R. *Langmuir* **1998**, *14* (7), 1759–1768.
(34) Sung, M. M.; Kluth, G. J.; Yauw, O. W.; Maboudian, R. *Langmuir* **1997**, *13* (23), 6164–6168.
(35) Demkov, A. A.; Navrotsky, A.; Frank, M.; Chabal, Y. In *Materials Fundamentals of Gate Dielectrics*; Springer: Dordrecht, The Netherlands: 2005; pp 367−401.
(36) Frank, M. M.; Chabal, Y. J.; Wilk, G. D. In *MRS Proceedings*, Vol. 745; Gardner, M. I., De Gendt, S., Maria, J.-P., Stemmer, S., Eds.; Materials Research Society: Warrendale, PA, 2002; Paper No. N2.4.
(37) Dai, M.; Kwon, J.; Halls, M. D.; Gordon, R. G.; Chabal, Y. J. *Langmuir 26*, (6), 3911−3917.
(38) Chesnokova, T. A.; Zhezlova, E. V.; Kornev, A. N.; Fedotova, Y. V.; Zakharov, L. N.; Fukin, G. K.; Kursky, Y. A.; Mushtina, T. G.; Domrachev, G. A. *J. Organomet. Chem.* **2002**, *642* (1−2), 20–31.
(39) Michalak, D. J.; Amy, S. R.; Aureau, D.; Dai, M.; Esteve, A.; Chabal, Y. J. *Nat. Mater. 9*, (3), 266-271.
(40) Yang, F.; Hunger, R.; Roodenko, K.; Hinrichs, K.; Rademann, K.; Rappich, J. *Langmuir* **2009**, *25* (16), 9313–9318.
(41) Fellah, S.; Teyssot, A.; Ozanam, F.; Chazalviel, J.-N.; Vigneron, J.; Etcheberry, A. *Langmuir* **2002**, *18* (15), 5851–5860.
(42) Saib, A. M.; Borgna, A.; van de Loosdrecht, J.; van Berge, P. J.; Niemantsverdriet, J. W. *J. Phys. Chem. B* **2006**, *110* (17), 8657–8664.
(43) Niemel, M. K.; Krause, A. O. I.; Vaara, T.; Kiviaho, J. J.; Reinikainen, M. K. O. *Appl. Catal., A* **1996**, *147* (2), 325–345.
(44) Schneider, R. L.; Howe, R. F.; Watters, K. L. *Inorg. Chem.* **1984**, *23* (26), 4593–4599.
(45) Rao, K. M.; Spoto, G.; Guglielminotti, E.; Zecchina, A. *J. Chem. Soc., Faraday Trans. 1* **1988**, *84*, 2195.
(46) Guglielminotti, E. *J. Mol. Catal.* **1981**, *13* (2), 207–214.
(47) Ang, H.-G.; Chuah, G.-K.; Jaenicke, S.; Loh, W.-L. *J. Chem. Soc. Dalton Trans.* **1997**, 1243–1250.
(48) Schore, N. E.; La Belle, B. E.; Knudsen, M. J.; Hope, H.; Xu, X. J. *J. Organomet. Chem.* **1984**, *272* (3), 435–446.
(49) Jemmis, E. D.; Pinhas, A. R.; Hoffmann, R. *J. Am. Chem. Soc.* **1980**, *102* (8), 2576–2585.